

A Mechanism for Data Quality Estimation of On-Body Cardiac Sensor Networks

Sunghoon Ivan Lee*, Charles Ling*, Ani Nahapetian*[†], Majid Sarrafzadeh*

*Computer Science Department

University of California Los Angeles

Los Angeles, USA

silee@cs.ucla.edu, czling@ucla.edu, ani@{cs.ucla.edu, csun.edu}, majid@cs.ucla.edu

[†]Department of Computer Science

California State University Northridge

Northridge, USA

Abstract—In this paper, we present a mechanism for estimating data quality of BANs composed of cardiac sensors. Currently available cardiac monitoring sensors suffer from high level of noise generated from loose physical contact of the sensor node due to the highly mobile and pervasive environment of the BAN (e.g., at-home remote health care applications). Therefore, there is a need to estimate the data quality of individual cardiac sensors as well as the data quality of the overall BAN while particularly considering the resource scarceness of BAN-scale mobile systems. The proposed method successfully estimates the data quality of a BAN without employing computationally expensive machine learning techniques. It also provides a number of resource management options that enable efficient data quality estimation. We present experimental results of four participants with three off-the-shelf cardiac sensors to form a BAN. We also present simulation results to examine if the proposed mechanism can successfully detect health hazardous events such as heart arrhythmia.

Keywords-Data quality; Cardiac Sensor; Body Area Network; Personal Area Network; Mobile Health Monitoring System

I. INTRODUCTION

Body area networks (BANs), or personal area networks (PANs), involve many applications that collect and process data from wearable and non-invasive sensors at different parts of the body. Among these currently available sensors, cardiac-monitoring sensors are the most common and widely used sensors. For example, in the survey on wearable sensor-based systems for health monitoring in [17], 90% (36 / 40) of the introduced commercial and research-based systems involve cardiac monitoring sensors. Cardiac sensors provide efficient bedside metric to assess the user's physical condition and thus, they are widely used in various fields such as medicine, sports and entertainment.

However, current wearable cardiac sensors have major problems that they often suffer from high level of noise in their data. This noise can be generated from (i) channel noise produced by human body [11], [19], (ii) noise caused by environments [5], and (iii) loose physical contact of the sensor node to the human body [13]. Among these various types of noise, the noise created by the loose contact of the sensor node has the greatest impact on the data quality. Motion artifacts of the user can cause physical vibration or detachment of the sensor nodes from the human body and significantly degrade the quality of sensor data, especially when the subject is highly

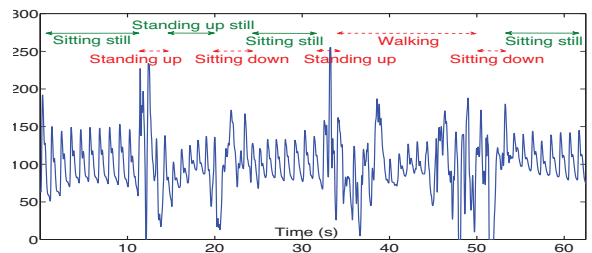


Fig. 1. A motivating example that shows human movement may corrupt the data from a wearable sensor. The data is obtained from one of our participants wearing an ECG sensor node at wrist

mobile (e.g., at-home remote health care applications). Fig. 1 illustrates a motivating example that shows noise generated by various motion artifacts. This signal was obtained from one of our participants wearing an on-body ECG sensor (Alive Heart Monitor [1]) at wrist. For example, walking involves relatively dynamic movements in arms and legs while relatively stable movements in chest and abdominal area. As a consequence, if the user has a single sensor at the wrist as in Fig. 1, the data would be highly corrupted when the user is walking. Therefore, multiple sensors are often mounted at different parts of the body to provide higher data quality. However, having multiple sensors on the body creates a challenging problem: which sensor produces the clean signal and which does not? In the field of medicine, it requires an extra manpower to review the data and filter out corrupted or dirty portion of the collected data [20], but this is not feasible in continuous and pervasive systems that we consider.

This paper introduces a mechanism for data quality estimation of a BAN composed of cardiac sensors. It provides a number of parameters that allow efficient utilization of the scarce resources of mobile systems. The proposed mechanism considers a BAN structure that all cardiac sensors transmit data to a single aggregator, and it runs in real-time with short latency for real-time applications such as remote health care or medical monitoring.

The remainder of this paper is organized as follows. In Section II, related works are discussed. The proposed mechanism is introduced in Section III. The experimental results and the conclusion is provided in Section IV and V, respectively.

II. BACKGROUND AND RELATED WORKS

Many studies have been performed on automatic classification of various cardiac signals. For example, in [8], various supervised and unsupervised methods for ECG classification are introduced. In [6], an ECG classification method based on a fuzzy clustering neural network is proposed. In [15], a method using a feature selection algorithm is investigated. However, all the aforementioned works involve computationally expensive machine learning algorithms. The textures and features used for the classification of a cardiac cycle vary dynamically according to the location of the sensor and the physical condition of the user. It implies that there exists no universal template for the classification, and the learning process must be frequently updated. Therefore these algorithms are not applicable to systems with scarce resources.

Recently, several approaches for estimating data quality for BANs has been studied and proposed. In [9] and [4], similar methods that detect the corruption of body sensor data are proposed. The methods investigate different features of medical signals such as amplitude, or temporal behavior to detect any changes made between the data transmitted from the sensor and the data received by the aggregator. These two approaches may work for channel noise or intrusion, but are not applicable when the noise is generated from the sensor node. In [7], a method to detect corrupted sensor data among multiple cardiac sensors in a BAN is proposed. However, authors assume that the blood pressure waveform is the bedside ground truth measurement that always provides uncorrupted signal. Thus, this cannot be applied to the model that we consider where none of the sensors is invulnerable.

III. PROPOSED MECHANISM

This section discusses the proposed mechanism that estimates the data quality of a BAN of cardiac sensors while particularly considering the resource scarceness. First, the proposed method filters out most of the normal events and recognizes any abnormal events (e.g., motion artifact noise or health hazardous events) at individual sensors. We define this step as the *local data quality estimation*. The second step is referred to as *global estimation* that aggregates information about the local data quality from all sensors and fuses the information in order to estimate the data quality of the overall BAN.

A. Local Data Quality Estimation

The objective of the local estimation is to detect any abnormal events in data generated from a single cardiac sensor. This mechanism is based on a well known fact that amplitude of cardiac signal and interpulse interval (IPI) variability are effective bedside measurements to detect any abnormal events [4], [8], [9]. The overview of the local estimation is illustrated in Fig. 2. First, the raw cardiac signal goes through a cardiac-cycle-locating process to partition the signal into cardiac cycles. This process starts with a sequence of cascaded linear digital filters that performs the pre-processing on the raw cardiac signal before the peak detection process. The three

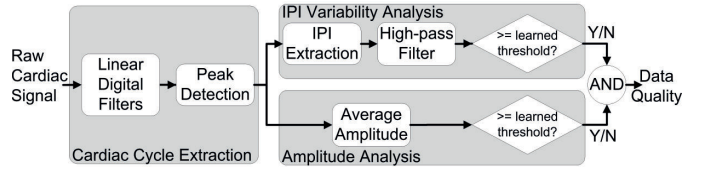


Fig. 2. The overview of the local data quality estimation

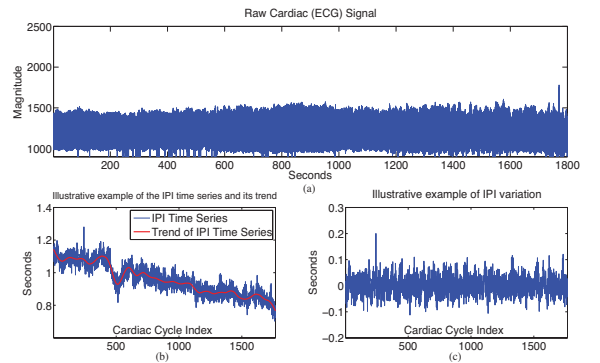


Fig. 3. (a) Raw cardiac (ECG) signal (b) The IPI time series with its trend (c) The high-pass filtered IPI time series (IPI variation)

filters include (i) an integer coefficient band-pass filter, (ii) a derivative filter combined with an amplitude squaring process, and (iii) a moving-window integrator [16]. The band-pass filter rejects unnecessary noise and the derivative filter provides the slope information of the filtered signal. The amplitude squaring process makes all data points positive and emphasizes the high amplitudes to make the peak detection easier. The moving-window integrator provides various waveform feature information in addition to the slope information. Then, the filtered signal goes through a peak detection logic similar to [18], which locates cardiac cycles.

Using the information about the location of cardiac cycles, we extract the time length of each cardiac cycle (i.e., IPI) and the average amplitude of each cardiac cycle. The time series of IPI is further filtered out using a high-pass filter to remove the trend as shown in Fig. 2. We define this high-pass filtered IPI time series as *IPI variation* and denote it as $v[n]$ (in seconds) where n is the index of cardiac cycles. Fig. 3 provides illustrative examples of the raw cardiac signal, its IPI time series with the trend, and the IPI variation of a 30 minute ECG signal of MIT-BIH Arrhythmia Database from PhysioNet [10]. The time series of average amplitude of cardiac cycles is denoted as $a[n]$.

We can interpret the data quality estimation as a binary classification (i.e., normal or abnormal cycle) using two continuous feature values (IPI and average amplitude), and employ the famous Bayes decision rule using the likelihood ratio. However, likelihood of the feature values given an abnormal cardiac cycle is very difficult to define since its distribution highly depends on different movements of the user. Thus, the proposed mechanism focuses on discarding most of normal cardiac cycles based on observing irregular

fluctuation in $v[n]$ and $a[n]$. Irregular fluctuation is a term that describes erratic movements in a time series that follow no recognizable or regular pattern [5]. It is known that health hazardous events carry irregular fluctuation in $v[n]$ and/or $a[n]$ [14]. Moreover, our observation (Section IV-A) verifies that motion artifact noise also carries irregular fluctuation in $v[n]$ and/or $a[n]$. Therefore, the pattern of normal cycles is defined by the degree of variation in normal $v[n]$ and $a[n]$ within a window size of N assuming that they have Gaussian distributions. It is known that the distributions of normal cardiac cycles are usually skewed rather than Gaussian [12]. However, distribution models for IPI variation are usually represented using very complicated models. More importantly, the models may evolve over time. Since our objective is to discard most of normal cardiac cycles rather than accurately modeling the distribution, we employ Gaussian distribution in our mechanism. Then, the pattern learning process involves computing the mean and the standard deviation of *normal cycles* for a window size of N . We define μ_v and σ_v as the mean and standard deviation of $v[n]$, and μ_a and σ_a as those of $a[n]$. The computational complexity of the learning process is bounded by $O(N)$ as it takes N summations to compute the mean and the standard deviation, and local memory is required to store N numbers. Therefore, the size of the window N provides design flexibility reflecting the available resources (i.e., memory or battery power). Moreover, this simple learning process can be frequently updated depending on the available resources. In summary, the proposed mechanism determines that the newest cardiac cycle of index n has high data quality if the following condition is satisfied:

$$\begin{aligned} \mu_v - \delta_v \cdot \sigma_v \leq v[n] \leq \mu_v + \delta_v \cdot \sigma_v \quad \text{AND} \\ \mu_a - \delta_a \cdot \sigma_a \leq a[n] \leq \mu_a + \delta_a \cdot \sigma_a. \end{aligned} \quad (1)$$

The above equation examines if the $v[n]$ and $a[n]$ of the new cardiac cycle is within the range of δ standard deviation from the mean of the past N normal data. The parameter δ must be greater than zero, and the value must be carefully selected because small δ may result in very low detection accuracy and large δ may result in high false negative. The data quality is defined as

$$Q[n] = \begin{cases} 1, & \text{if (1) is satisfied} \\ 0, & \text{otherwise} \end{cases}. \quad (2)$$

The output of the local estimation, which is transmitted to the aggregator, is a two-tuple: $\langle v[n], Q[n] \rangle$. $v[n]$ is used to synchronize the $Q[n]$ among various sensors.

In order to initiate the automatization of the estimating processes, the system needs N normal cycles to learn the normal patterns. For instance, in the experiments in Section IV-A, we asked the participants to sit on a chair without any movements to acquire $N = 20$ normal cycles at the beginning. Then, δ_v and δ_a are chosen such that all N normal cycles satisfy (1) and multiply those values by 1.5 to allow sufficient room. Moreover, μ and σ can be updated on-the-fly using the cardiac cycles that are determined to be normal based on the results of (2).

In summary, the local process estimates the data quality of individual cardiac sensors with computationally efficient learning process. The local process provides resource management options for mobile systems such as (i) the learning window size N and (ii) the frequency of updating the learning process.

B. Global Data Quality Estimation

The data fusion process is performed at the aggregator side. It collects the information about the estimated data quality from each sensor node and analyzes the data to estimate the data quality of the overall BAN. Suppose the aggregator is associated with K sensor nodes. Let us denote the IPI variation and the quality information of the k^{th} sensor node as $v_k[n]$ and $Q_k[n]$, respectively. The first step taken at the aggregator side is to generate a new time series, $t_k[m]$. In order to compute $t_k[m]$, we synchronize the temporal domain of all sensors using the minimum sampling rate of the sensors: $r^* = \min(r_k)$ for $1 \leq k \leq K$. The two equations used to synchronize the time domain are defined as

$$\begin{aligned} v'_k[n] &= \lceil v_k[n] \cdot r^* \rceil, \text{ and} \\ v''_k[n] &= v''_k[n-1] + v'_k[n], \end{aligned}$$

assuming that $v''_k[0] = 0$. Note that $v'_k[n]$ is just a time series of $v_k[n]$ multiplied to the minimum sample rate, and $v''_k[n]$ is the cumulated time series of $v'_k[n]$ in order to denote the synchronized time index for each cardiac cycle. Then, $t_k[m]$ is defined as

$$t_k[m] = Q_k[n] \text{ for } v''_k[n-1] < m \leq v''_k[n].$$

The above equation creates a time series for the k^{th} sensor that shows the quality of a cardiac cycle for the *length* of that cardiac cycle, where this length is synchronize among K sensors. Note that the value of $t_k[m]$ is binary since the value of $Q[n]$ is binary, that is, $t_k[m] = 1$ when the data quality is high and $t_k[m] = 0$ otherwise.

Next, we fuse the synchronized $t_k[m]$ to estimate the data quality $t[m]$ of the overall BAN using a majority voting function that defines $t[m] = 1$ when the majority of $t_k[m] = 1$. Then, $t[m]$ estimates the data quality of the BAN consists of multiple cardiac sensors. The index m such that $t[m] = 1$ indicates the time instance where the data quality of BAN is high. On the other hand, m such that $t[m] = 0$ indicates the time instance where none of the on-body sensors provides clean cardiac signals.

IV. EXPERIMENTAL RESULTS

In this section, we present experimental results and simulation results to show that the proposed mechanism can successfully estimate the data quality without using computationally expensive classifier algorithms. In Section IV-A, we present results of experiments conducted on four participants to show that the proposed mechanism recognizes the noise created by motion artifacts. Moreover, in Section IV-B, we perform a simulation on multi-variable cardiac data in order address that the proposed mechanism can recognize the noise created by health hazardous events such as heart arrhythmia.

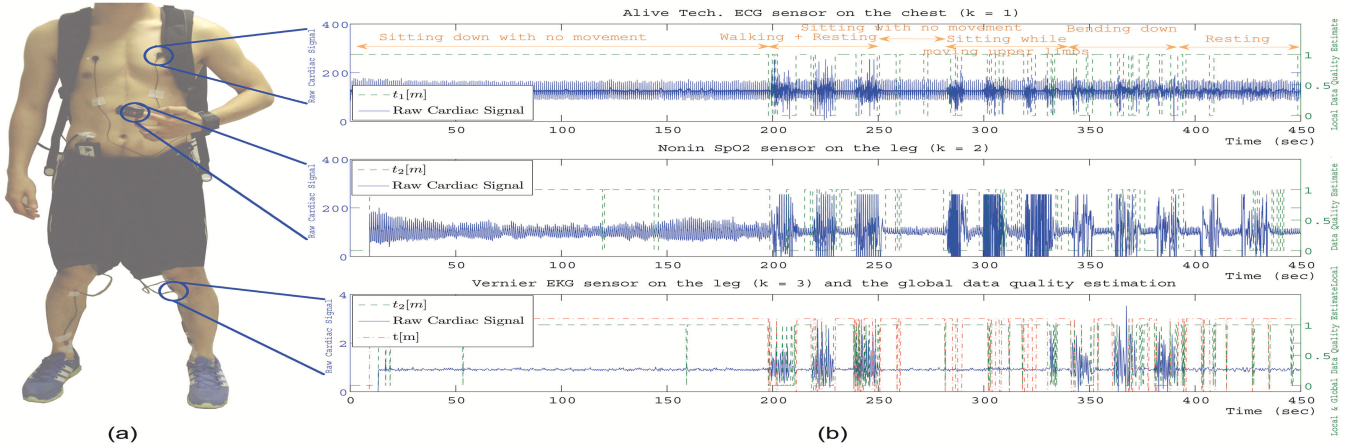


Fig. 4. (a) The experimental setup for participants. (b) The raw signal and $t_1[m]$ for Alive Heart Monitor located at the chest with annotation of the performed actions in orange color (top), the raw signal and $t_2[m]$ for Nonin Pulse Oximeter located at the finger (middle), and the raw signal and $t_3[m]$ for Vernier EKG Sensor located at the leg (bottom). The bottom graph also includes the fused data quality estimation $t[m]$ in red color

A. Noise from Motion Artifacts

This section presents the results of experiments conducted on four participants wearing three off-the-shelf cardiac sensors (i.e., $K = 3$). Participants are recruited on the campus of University of California Los Angeles, all males at ages between 19 and 32. The cardiac sensors used in the experiment include two ECG sensors and a pulse oximeter (SpO_2): Alive Heart Monitor [1], Vernier EKG Sensor [3], and Nonin Onyx 9560 [2]. The Alive Heart Monitor is placed on the chest, the Vernier EKG sensor on the leg, and the Nonin Onyx 9560 on the left index finger as shown in Fig. 4 (a). All three devices are connected to a single aggregator in the backpack (i.e., portable laptop PC). Each participant is asked to repeat a set of actions that simulates the average daily activity of a person based on the American Time User Survey (ATUS) 2009 [21]. Participants performed the following actions in a sequential order: walking, sitting down with no movement, sitting down while moving upper limbs, bending down to pick up an object, and standing up while moving upper limbs. For example, walking can simulate general walking, or vacuuming. Sitting down while moving upper limbs simulates eating, office working, or watching TV. For each action in the set, we asked the participants to perform the action for 10 seconds and rest for another 10 seconds to clearly distinguish the noise from normal signal, and repeat this combination of action and rest three times. We manually annotated all cardiac cycles to be either normal or abnormal (noise), and compared the detection results (i.e., $t_k[m]$) against this ground truth annotation for each sensor data. We also fused the data from three sensors using a majority voting function and evaluated the detection results of the overall BAN (i.e., $t[m]$). Note that the ground truth annotation for the overall BAN is also generated by a majority voting mechanism among the ground truth annotations of individual sensor data. The value of N used in this experiment is 20, and the values of parameters δ_v and δ_a computed for Alive Heart Monitor are 4.05 and

5.29, respectively. For Nonin Onyx, $\delta_v = 2.67$ and $\delta_a = 2.54$, and for Vernier EKG Sensor, $\delta_v = 3.25$ and $\delta_a = 4.13$. The learning process is performed at the beginning of the experiment when the first 20 samples are collected. Then, the learning process is updated once when the participants are asked to rest for 20 seconds after the walking phase. The experimental results of one of the participants P_1 are provided in Fig. 4 (b). Fig. 4 (b) illustrates data streams obtained from chest ($k = 1$), finger ($k = 2$) and leg ($k = 3$) with the local data quality estimation results $t_k[m]$. The global data quality estimation $t[m]$ is provided in the bottom graph in red. In this experiment, a total 531 cardiac cycles are evaluated.

The experimental results are evaluated using (i) the overall detection rate (r_d), (ii) false abnormal rate (r_{fa}), and (iii) false normal rate (r_{fn}). Table I shows these results of the three local estimations and the global estimation. We see that the overall detection rate, false abnormal rate and false normal rate are improved when the signals are fused together. Among four participants, the average detection rate was 0.9056, the average false abnormal rate was 0.0389, and the average false normal rate was 0.2511. The false normal rate was relatively high because the IPI and the average amplitude sometimes fell into the inequality (1). However, the proposed mechanism successfully detected the *presence* of abnormality due to an action taken for 10 seconds with 100% accuracy.

B. Noise from Health Hazardous Events

Due to the limitation and safety issues in recruiting participants with severe cardiac ailments who are likely to undergo a health hazardous cardiac problem during the experiment, we perform a simulation of the proposed mechanism on the existing public database in order to test the proposed mechanism on hazardous health events. The database used in this simulation is the MGH/MF Waveform Database from PhysioNet [10], which includes three ECGs, an arterial pressure, a pulmonary arterial pressure, and a central venous pressure signal. This multi-dimensional cardiac data collected from various parts

TABLE I

THE EXPERIMENTAL RESULTS THAT SHOW THE OVERALL DETECTION RATE, FALSE ABNORMAL RATE, AND FALSE NORMAL RATE FOR THE THREE LOCAL DATA QUALITY ESTIMATION AND THE GLOBAL ESTIMATION.

	Chest			Finger		
	r_d	r_{fa}	r_{fn}	r_d	r_{fa}	r_{fn}
P_1	0.8901	0.0650	0.3458	0.8441	0.1537	0.1602
P_2	0.8561	0.1222	0.3472	0.7255	0.0156	0.3180
P_3	0.8661	0.0367	0.2715	0.8375	0.0614	0.2646
P_4	0.8371	0.0728	0.3105	0.8004	0.1145	0.2712
Avg.	0.8624	0.0742	0.3188	0.8019	0.0863	0.2535
	Leg			Global		
	r_d	r_{fa}	r_{fn}	r_d	r_{fa}	r_{fn}
P_1	0.8427	0.0217	0.2967	0.9170	0.0434	0.2400
P_2	0.8029	0.2104	0.3403	0.9270	0.0375	0.2280
P_3	0.8361	0.0437	0.5787	0.8974	0.0224	0.3020
P_4	0.8221	0.0548	0.4813	0.9024	0.0523	0.2345
Avg.	0.8260	0.0827	0.4243	0.9056	0.0389	0.2511

of body can effectively imitate the signals from various on-body sensor nodes. The original dataset contains total 250 sets of cardiac signals, each containing 12 to 86 minutes of recording. We randomly chose 9 signal sets and performed the simulation. These signals include cardiac events such as premature ventricular contraction, supraventricular premature, and ectopic beat, which are all manually annotated by clinical professionals. Two interesting observations were made while investigating these signals. First, unlike the experiments we discussed in Section IV, all local signals had the same IPI time series since none of the sensors is locally distorted due to motion artifacts. Second, the average ratio of the number of normal cardiac cycles to the total number of cardiac cycles is 99.1%. It implies that a dummy algorithm always predicting the results to be normal cardiac cycles would achieve 99.1% accuracy. Thus, we investigate detection rate for normal and abnormal cycles separately. The value of N used in this simulation is 300, and $\delta_v = 2.54$ and $\delta_a = 2.02$ for all channels. The learning process is updated every 300 samples of IPI. The results of the simulation is summarized in the Table II.

In this simulation, a total 39760 cardiac cycles are extracted from approximately 300 minutes long cardiac signals. The total number of normal cardiac cycles and abnormal cardiac cycles are 35659 and 234 respectively. In average, the detection rate for the abnormal cycles is 100% and the detection rate for the normal cycles is 87.8%.

V. CONCLUSION

In this paper, we introduce a mechanism for estimating data quality of a BSN composed of cardiac sensors. The proposed method employs local and global estimation process in order to estimate the data quality of individual sensors and to fuse the information. We present experimental results based on three off-the-shelf cardiac sensor devices in order to detect motion artifact noise. We also present simulation results to detect health hazardous events using the proposed mechanism.

TABLE II

THE SIMULATION RESULTS THAT SHOW THE DETECTION RATE OF NORMAL AND HEALTH HAZARDOUS EVENTS USING THE PROPOSED MECHANISM

Dataset	N'_a	N_a	r_{fn}	N'_n	N_n	r_{fa}
03	22	22	0	1431	1569	0.088
45	50	50	0	4512	5708	0.210
105	31	31	0	4234	4536	0.067
107	24	24	0	3179	4031	0.211
139	18	18	0	4322	5015	0.138
162	16	16	0	4220	4680	0.098
186	23	23	0	2107	2334	0.097
217	40	40	0	3985	4150	0.039
227	10	10	0	3320	3535	0.087
Overall	234	234	0	31310	35659	0.122

REFERENCES

- [1] Alive Technologies, <http://www.alivetec.com>, 2011.
- [2] Nonin Medical Inc., <http://www.nonin.com>, 2011.
- [3] Vernier Technologies, <http://www.vernier.com>, 2011.
- [4] M. Ammen, A. Nessa, and K. Kwak. "QoS issues with focus on wireless body area networks. In *The International Conference on Communications and Information Technology (ICCIT 2008)*, pages 801–807, Busan, South Korea, November 2008.
- [5] B. Bowerman, B. O'Connell, and A. Koehler. *Forecasting, timeseries, and regression*. Thomson, fourth edition, 2005.
- [6] R. Ceylan, X. Ozbay, and B. Karlik. A novel approach for classification of ECG arrhythmias: Type-2 fuzzy clustering neural network. *Expert Systems with Applications*, 36:67216726, 2009.
- [7] G. Clifford, A. Aboukhalil, and et. al. Using the blood pressure waveform to reduce critical false ECG alarms. *Comput in Cardiol*, 33:829–832, 2006.
- [8] G. Clifford, F. Azuaje, and P. McSharry. *Advanced methods and tools for ECG data analysis*. Artech House, Norwood, MA, 2006.
- [9] A. Giani, T. Roosta, and S. Sastry. Integrity checker for wireless sensor networks in health care applications. In *Proceedings of the 2nd International Conference on Pervasive Computing Technologies for Healthcare, IEEE Computer Society*, pages 135–138, Tampere, Finland, 2008.
- [10] A. Goldberger, L. Amaral, and et. al. PhysioBank, PhysioToolkit, and PhysioNet: Components of a new research resource for complex physiologic signals. *Circulation*, 101(23):e215–e220, 2000 (June 13).
- [11] A. Johansson. Wave-propagation from medical implants-influence of body shape on radiation pattern. In *2nd Joint EMBS/BMES Conference*, Oct 2002.
- [12] R. Kitney and O. Rompelman. *The Study of Heart-rate Variability*. Oxford University Press, 1980.
- [13] J. Ko, L. Chenyang, and et. al. Wireless sensor networks for healthcare. *Proceedings of the IEEE*, 98(11), November 2010.
- [14] D. Lin and R. Hughson. Modeling heart rate variability in healthy humans: A turbulence. *Phys. Rev. Lett.*, 86:1650–1653, 2001.
- [15] T. Mar, S. Zaunseder, and et. al. Optimization of ECG classification by means of feature selection. *IEEE transactions on Biomedical Engineering*, 99, February 2011.
- [16] J. Pan and W. Tompkins. A real-time QRS detection algorithm. *IEEE Trans. Biomed. Eng.*, 32:230–236, 1985.
- [17] A. Pantelopoulos and N. Bourbakis. A survey on wearable sensor-based systems for health monitoring and prognosis. *IEEE Trans. on systems, man, and cybernetics*, 40(1), January 2010.
- [18] A. Ruha, S. Sallinen, and S. Nissila. A real-time microprocessor QRS detector system with a 1-ms timing accuracy for the measurement of ambulatory HRV. *IEEE Trans. Biomed. Eng.*, 44:159–167, 1997.
- [19] R. Shah, L. Nachman, and C. Wan. On the performance of Bluetooth and IEEE 802.15.4 radios in a body area network. In *Third International Conference on Body Area Networks (BodyNets'08)*, Tempe, AZ, March 2008.
- [20] H. Thomas, T. Helms, , and et. al. Telemetry in the clinical setting. *Herzschrittmachertherapie und Elektrophysiologie*, 19(3), August 2009.
- [21] US Bureau of Labor Statistics and US Census Bureau. American time use survey user's guide - Understanding ATUS 2009, 2011.